Organising Centres in the Semi-global Analysis of Dynamical Systems

Broer, H.W.; Naudot, V.; Roussarie, R.; Saleh, K.; Wagener, F.O.O.

Published in:
International Journal of Applied Mathematics and Statistics

International Journal of Applied Mathematics & Statistics,
Int. J. Appl. Math. Stat.; Vol. 12; No. D07; December 2007
ISSN 0973-1377 (Print), ISSN 0973-7545 (Online)

Organising Centres in the Semi-global Analysis of Dynamical Systems

H.W. Broer[1], V. Naudot[2], R. Roussarie[3], K. Saleh[4] and F.O.O. Wagener[5]

[1]Department of Mathematics, University of Groningen,
P.O. Box 800, 9700 AV Groningen, The Netherlands
broer@math.rug.nl

[2]Department of Mathematics, University of Warwick,
Coventry CV4 7AL, UK
vijnc@maths.warwick.ac.uk

[3]Institut Mathématiques de Bourgogne,
CNRS, 9, avenue Alain Savary,
B.P. 47 870, 21078 Dijon cedex, France
roussarie@u-bourgogne.fr

[4]Department of Mathematics, University of Groningen,
P.O. Box 800, 9700 AV Groningen, The Netherlands
khairul@math.rug.nl

[5]CeNDEF Dept of Quantitative Economics, University of Amsterdam
Roetersstraat 11 1018 WB Amsterdam, The Netherlands
wagener@uva.nl

ABSTRACT

The notion of organising centre of a bifurcation diagram is used as an ordering principle in the analysis of nonlinear problems in pure and applied dynamical systems theory. When considering a given, generic n-parameter family of dynamical systems the codimension n bifurcations are isolated in the parameter space, generating a more global array of lower codimension bifurcations. It often makes sense to add one extra parameter to the system, e.g., by varying a 'constant' coefficient. In such cases, semi-global parts of the given n-dimensional bifurcation set can be understood as generic slices in versal unfoldings of codimension $n+1$ singularities. This can give great insight in the structure of the given system, as we shall illustrate in two extensive case studies.

Keywords: Organising Centre, Bifurcations, Predator-prey Model, Normal-internal Resonance.

2000 Mathematics Subject Classification: 58K45, 37C10, 34C23.

1 Introduction

Singularity Theory and Catastrophe Theory as originated by Whitney, Thom and Arnold [82, 94, 7, 8, 92] are known to have wide applications in the field of dynamical systems and beyond.

In particular this holds for modelling problems where 'system parameters' play a role. An important example, which also is the focus of the present work, concerns bifurcation theory. The theoretical studies of bifurcations deal with so-called universal problems. This means that sufficiently many parameters are available for (uni-) versality of generic families of dynamical systems in the context at hand, under a relevant equivalence relation. This has led to the classification of generic, local bifurcations as reported in, e.g., [5, 52, 63, 43].

In many applications models have a certain number, say n, of parameters. Moreover, the bifurcation analysis, taking place in the product of phase space and parameter space, is not restricted to local features only. On the contrary, often the interest is the global organisation of the parameter space regarding bifurcations, which can be both local and global. Here global bifurcations refer to homoclinic and heteroclinic tangencies [72], or to periodic and quasi-periodic bifurcations [16, 23]. The present work focuses on the (semi-) global organisation of the parameter space in terms of local bifurcations. Generically we only meet bifurcations of codimension not exceeding the given number n of parameters. The bifurcations of codimension n correspond to isolated points in the parameter space and these act as organising centres of the bifurcation diagram, according to the principle of Singularity Theory. With V.I. Arnold ([8], Part II. *Catastrophe Theory*) we say: "*It may be that the most astounding conclusion from the large number of 'classification' problems in singularity and bifurcation theory is that a comparatively small list of standard forms (the cusp (semi-cubical), the swallowtail, ...) turns out to be universal, and serves in a large number of different theories, between which, at first glance, no connection at all is present.*"

The main interest of this research is the following. In many examples the (semi-) global array of codimension n points (and their connections) is generated by one or more codimension $n+1$ bifurcation points outside the given family, but in a certain sense 'near' to it. This can be made clear by adding a suitable extra parameter to the family (often one of the coefficients of the model). The given family then can be viewed as a generic n-dimensional section or slice in a $(n+1)$-dimensional parameter space. Compare with the so-called 'path formalism' [49, 50]. As we shall illustrate by our examples, the codimension $n+1$ points then generate the array of codimension n bifurcations in a semi-global or even global way; in this way the bifurcations of codimension less than or equal to n are subordinate to one or more codimension $n+1$ singularities. Colloquially we say that they act as 'organising centres', also compare with [31, 32, 33, 34, 95, 61, 85]. To fix thoughts consider the following example.

(Organising Centre) A two-parameter family with cusps and folds, as they occur in the catastrophe set of the two-parameter family of functions [7, 82, 94]

$$f_{\kappa,\eta}(x) = x^5 + bx^3 + \kappa x^2 + \eta x,$$

where $x \in \mathbb{R}$ and where $\eta, \kappa \in \mathbb{R}$ are parameters. Recall that the catastrophe set of a family of functions is given by the projection of the set of singular points (i.e. points for which $f'_{\kappa,\eta}(x) = 0$) on the parameter space. Figure 1(a) shows the catastrophe set for the case that $b > 0$: two

cusp points are joined by three fold curves. In the case $b < 0$ (not shown), there is just a single fold curve in the form of a parabola.

If we consider b to be a parameter as well, then Figure 1(a) is a slice of the three-dimensional catastrophe set of the family, which has a swallowtail bifurcation occurring at $(\kappa, \eta, b) = (0, 0, 0)$ as organising centre; see Figure 1(b).

Catastrophe theory deals with critical points of real functions, but the above idea applies just as well within the context of local bifurcations of vector fields, where the codimension 0 strata contain Morse-Smale dynamics, e.g., compare with [71, 43]. For similar examples see below. For an interpretation of the present example in an optimisation problem, see §5.

A second message that we shall touch upon more briefly is the complication of the bifurcation geometry by resonances. To fix thoughts, consider an autonomous model, where the coefficients are made time-periodic or quasi-periodic in a perturbative way. In practice this situation often is attained by a normalisation or averaging process. Our claim is that the dynamics and bifurcation geometry of the autonomous 'principal part' in the product of phase- and parameter space is complicated and fine-structured by perturbative (quasi-) periodicity. Generically, this occurs in a way that is theoretically predictable. Here key notions are Cantorisation of bifurcation diagrams in the product of phase- and parameter space, and in particular the fraying of certain bifurcation boundaries, c.f. [15, 24, 23, 20, 18, 22, 54, 88, 75].

2 A Predator-prey Model

The first example consists of a particular family of planar vector fields, which models the dynamics of the populations of predators and their prey in a given ecosystem, and which is a variation on the classical Volterra-Lotka system [65, 86]. For the latter system the change of the prey density per unit of time per predator, called the *response function* [76], is proportional to the prey density. This means that there is no saturation of the predator when the amount of available prey is large. However, it is more realistic to consider a nonlinear and bounded response function, and in fact different response functions have been used in the literature to model the predator response, see [3, 12, 55].

For instance, Zhu et al. [95] have studied recently the following predator-prey model

$$\begin{cases} \dot{x} &= x(a - \lambda x) - yP(x) \qquad \text{(prey)}, \\ \\ \dot{y} &= -\delta y + yQ(x) \qquad\quad \text{(predator)}. \end{cases} \tag{2.1}$$

The variables x and y denote the density of the prey and predator populations respectively, while $P(x)$ is a non-monotonic response function [2] given by

$$P(x) = \frac{mx}{\alpha x^2 + \beta x + 1}, \tag{2.2}$$

where α, m are positive and where $\beta > -2\sqrt{\alpha}$. Observe that in the absence of predators, The number of prey increases according to a logistic growth law. The coefficient a represents the intrinsic growth rate of the prey, while $\lambda > 0$ is the rate of competition or resource limitation of prey. The natural death rate of the predator is given by $\delta > 0$. In Gause's model [48] the function $Q(x)$ is given by $Q(x) = cP(x)$, where $c > 0$ is the rate of conversion between prey and predator. For further discussion on the biological relevance of the model see [75, 29, 95, 74].

In this section, we investigate the following family

$$\begin{cases} \dot{x} &= x\left(1 - \lambda x - \dfrac{y}{\alpha x^2 + \beta x + 1}\right) \qquad \text{(prey)}, \\ \\ \dot{y} &= y\left(-\delta - \mu y + \dfrac{x}{\alpha x^2 + \beta x + 1}\right) \qquad \text{(predator)}, \end{cases} \tag{2.3}$$

where $\alpha \geq 0,\ \delta > 0,\ \lambda > 0,\ \mu \geq 0$ and $\beta > -2\sqrt{\alpha}$ are parameters. We note that (2.3) is obtained from (2.1) by adding the term $-\mu y^2$ to the second equation and after scaling x and y, as well as the parameters and the time t. In this way we take into account competition between predators for resources other than prey, see [10, 11]. The non-negative coefficient μ is the rate of competition amongst predators.

Our goal is to understand the structurally stable dynamics of (2.3) and in particular the attractors with their basins where we have a special interest for multi-stability. We investigate the bifurcations between the open regions of the parameter space that concern such dynamics, thereby giving a better understanding of the family.

We also address the modification of this system where a small parametric forcing is applied in the parameter λ, as suggested by Rinaldi et al. [73]. We put

$$\lambda = \lambda(t) = \lambda_0\left(1 + \varepsilon \sin\left(\frac{2\pi}{w}t\right)\right), \tag{2.4}$$

where $\varepsilon < 1$ is a perturbation parameter and w is a constant. We shall discuss how this modification effects the results for the autonomous system (2.3), which then serves as principal part of the forced system. We are particularly interested in the occurrence of 'large scale' strange attractors.

Remark 2.1. In addition to (2.4), we could also have set

$$a = a(t) = a_0\left(1 + \varepsilon \sin\left(\frac{2\pi}{w}t\right)\right),$$

which models seasonal growth rate fluctuations, see for instance [73]. More generally, the periodic forcing terms may be replaced by quasi-periodic terms.

2.1 Sketch of Results

In what follows we describe the results on the autonomous system (2.3).

Trapping domains and Reduced Morse-Smale portraits. The investigation concerns the dynamics of (2.3) in the closed first quadrant $\mathrm{clos}(\mathcal{Q})$ where $\mathcal{Q} = \{(x, y) \in \mathbb{R}^2 | x > 0,\ y > 0\}$ with boundary $\partial\mathcal{Q}$, which are both invariant under the flow. We shall show that system (2.3) has a compact *trapping domain* $\mathcal{B}_p \subset clos(\mathcal{Q})$: all orbits in $clos(\mathcal{Q})$ enter $\mathcal{B}_p$ after finite time and do not leave it again. For the moment we restrict the attention to structurally stable (or Morse-Smale) dynamics. In the interior of $\mathcal{B}_p$, there can be at most two stable equilibria and possibly one saddle-point. We study these singular points using algebraic tools, occasionally supported by computer algebra. Also we numerically detect several cases with one or two limit cycles. Here we often use numerical continuation, where algebraic detection of Hopf or Bogdanov-Takens bifurcations helps to initiate the continuation process.

Since limit cycles are hard to detect mathematically, our approach is to reduce, by surgery, the structurally stable phase portraits to new portraits without limit cycles. During surgery we change a part of the phase space by smooth cutting and pasting [66, 69]. Next, with the help of topological means (Poincaré-Hopf Index Theorem, Poincaré-Bendixson Theorem [66, 71]) we find a complete classification that is of great help to understand the original system (2.3). Compare with Figure 2.

Notation	Name	Incidence
TC_1	Transcritical	
TC_2	Degenerate transcritical	$SN_1 + TC_1$
TC_3	Doubly degenerate transcritical	SN_2 + TC_2
PF_1	Pitchfork	
PF_2	Degenerate pitchfork	$PF_1 + SN_1$
SDZ_2	Symmetric double zero	$PF_1 + H_1$
SN_1	Saddle-node	
SN_2	Cusp	$SN_1 + SN_1$
BT_2	Bogdanov-Takens	$SN_1 + H_1 + L_1$
BT_3	Degenerate Bogdanov-Takens	$BT_2 + H_2 + DL_2$
NF_3	Singularity of nilpotent-focus type	$SN_2 + BT_2 + L_2 + H_2$
NE_3	Singularity of nilpotent-elliptic type	$SN_2 + BT_2 + L_2 + H_2$
H_1	Hopf	
H_2	Degenerate Hopf	$H_1 + SNLC_1$
L_1	Homoclinic (or Blue Sky)	
L_2	Homoclinic at saddle-node	$L_1 + SN_1$
DL_2	Degenerate homoclinic	$L_1 + SNLC_1$
$SNLC_1$	Saddle-node of limit cycles	
HE_1	Heteroclinic	

Table 1: List of bifurcations occurring in systems (2.3), (3.6) and (3.7). This notation will be kept throughout. All bifurcations are local except the latter five, which are global. In all cases the subscript indicates the codimension of the bifurcation. In the column 'Incidence' we put the subordinate bifurcations of the highest codimension. See [1, 43, 44, 52, 63] for details concerning the terminology and fine structure.

Organization of the parameter space. Our main interest is the dense-open subset of the parameter space $^5 = \{\alpha, \beta, \mu, \delta, \lambda\}$ with structurally stable dynamics. The complement of this

set is the bifurcation set, which consists of strata of different codimension.

It turns out that the parameters δ and λ play a minor role and that we can describe the bifurcation set as follows. Let $\Delta = \{(\delta, \lambda) \in \mathbb{R}^2 | \delta > 0, \lambda > 0\}$ and $\mathcal{W} = \{(\alpha, \beta, \mu) \in \mathbb{R}^3 | \alpha \geq 0, \beta > -2\sqrt{\alpha}, \mu \geq 0\}$. We fix $(\delta, \lambda) \in \Delta$ and bifurcations of (2.3) are described in the space $\mathcal{W}$. To discuss this we introduce the projection

$$\Pi : \mathcal{W} \times \Delta \to \Delta, \, (\alpha, \beta, \mu, \delta, \lambda) \mapsto (\delta, \lambda),$$

studying all fibers $\Pi^{-1}(\delta, \lambda)$. This argument works as long as the fibers are transversal to the bifurcation set consisting of singularities of nilpotent-focus type (NF_3), in which case we only have to consider bifurcations of codimension less than or equal to 3. It turns out that this is the case in the complement of a smooth curve $\mathcal{C}$ in Δ, compare with Figure 3(a). Indeed the bifurcation set in $\mathcal{W}$, up to diffeomorphisms, is constant above each open region Δ_1 and Δ_2, separated by $\mathcal{C}$, see [27, 28, 29]. Above the curve $\mathcal{C}$ there is a folding of the bifurcation set whenever the fiber $\Pi^{-1}(\delta, \lambda)$ is tangent to it.

When restricting to Δ_1 and Δ_2 the codimension 3 bifurcations in $\mathcal{W}$ act as organising centres. This means that when taking two-dimensional sections in $\mathcal{W}$ we see a semi-global picture organized by the trace of the codimension 3 bifurcations, compare with [29]. For each region Δ_1 and Δ_2 the associated bifurcation set in $\mathcal{W}$ is depicted in Figure 3(b) and Figure 3(c), respectively. Figure 3(c) shows that the bifurcation set possesses several codimension 2 curves subordinate to four codimension 3 points which act as organising centres. Now we explain how to understand the bifurcations up to codimension 1.

Organising centres and two-dimensional bifurcation diagrams. Given the organising centres of the bifurcation sets in $\mathcal{W}$, we take two-dimensional sections $\mathcal{S}_i$, $i = 1, \ldots, 6$, transversal to the codimension 2 curves as indicated in Figure 3. Each two-dimensional section intersects codimension 0 strata in several open regions separated by codimension 1 curves. The two-dimensional bifurcation diagrams are depicted, emphasising the basins of attraction and the possible multi-stability.

We illustrate our strategy in Figure 4 by presenting one of the two-dimensional bifurcation diagrams (in $\mathcal{S}_1$). For the other two-dimensional diagrams see [29, 74].

Limit cycles and homoclinic loops. Limit cycles may be created by Hopf bifurcations (H_1) (see for instance regions 1 and 7 of Figure 4, by saddle-node bifurcations of limit cycles ($SNLC_1$) (see regions 9 and 11 of the same Figure 4 and by homoclinic bifurcations (L_1) (or Blue Sky catastrophe [1], see regions 1 and 12 in Figure 4. The occurrence of limit cycles is investigated numerically (continuation) with help of Matlab [53], Matcont [51] and AUTO [42].

As said before, all local bifurcations can be detected algebraically, which is not the case for the global bifurcations L_1 and $SNLC_1$. Again we resort to numerical continuation methods, using various codimension 2 bifurcations to create initial data. For example, in Figure 4, the

degenerate Hopf bifurcation H_2 'generates' the curve $SNLC_1$, while the Bogdanov-Takens bifurcation BT_2 'generates' the curve L_1^a.

2.2 Parametric forcing

Dynamical properties of system (2.3) with parametric forcing (2.4) can be expressed in terms of the stroboscopic map

$$\mathcal{P}_\varepsilon : \mathbb{R}^2 \to \mathbb{R}^2, \quad (x, y) \mapsto \varphi_\varepsilon^1(x, y), \tag{2.5}$$

where φ_ε^t denotes the flow of the time-periodic system written as a three-dimensional vector field $X_\varepsilon = X_\varepsilon(x, y, t; \alpha, \beta, \mu, \delta, \lambda)$. Fixed points of $\mathcal{P}_\varepsilon$ correspond to periodic solutions of X_ε with period w, and similarly invariant circles of $\mathcal{P}_\varepsilon$ correspond to invariant 2-tori of X_ε.

We discuss here the general relationship between the autonomous system X_0, which here plays the role of principal part, and the time-periodic perturbation X_ε for $|\varepsilon|$ small. A number of dynamical properties of $\mathcal{P}_\varepsilon$ are considered, as these follow from more or less classical perturbation theory [4, 30, 31, 52]. First of all hyperbolic periodic points (including fixed points) of $\mathcal{P}_0$ persist for $\mathcal{P}_\varepsilon$, for $\varepsilon \ll 1$, as well as their local stable and unstable manifolds. We note that globally the stable and unstable manifolds generically will behave different by separatrix splitting, giving rise to (transversal) homoclinic and heteroclinic tangles. Secondly, local bifurcations are persistent. In particular, this holds for saddle-node and cusp bifurcations of periodic points but also for the Hopf bifurcations of these periodic points. In the latter case (for which the three-dimensional vector field X_ε gives Neĭmark-Sacker bifurcations), we encounter resonances due to the interaction of internal ('natural') and forcing frequencies. The strong resonances are more involved [4, 30, 31, 59, 73, 81], but in the case of weak resonances, near the Hopf curve, the limit cycle turns into a $\mathcal{P}_\varepsilon$-invariant circle. In a corresponding three-dimensional section in $\mathcal{W}$, the associated rotation number is rational in a dense-open array of Arnol'd tongues emanating from the Hopf curve. Here the circle dynamics is of Kupka-Smale type [71], which corresponds to frequency locking with periodic forcing. For a large measure set outside the tongues the invariant circles are quasi-periodic with Diophantine rotation number. The invariant circles break up further away from the Hopf curve in a complicated way, compare with [30]. The saddle-node bifurcation of limit cycles in X_0 turns into a quasi-periodic saddle-node bifurcation for $\mathcal{P}_\varepsilon$ [23, 24] with all the ensuing dynamical complexity [38, 39, 40], also compare with [26]. In a systematic study of the attractors of $\mathcal{P}_\varepsilon$ as a function of the parameters, we expect the same complexity as described in [25, 30, 31], for more background also compare with [67, 72]. In this investigation the present study of the autonomous system provides a skeleton.

In this section we restrict to the numerical detection of a few attractors of $\mathcal{P}_\varepsilon$ near homoclinic connections in the autonomous system X_0. More precisely we consider the two-dimensional bifurcation diagrams of X_0, looking for the loci of homoclinic orbits (L_1 in Figure 4 and L_1^a, L_1^b in Figure 4. These loci can be continued in the ε-direction for $\varepsilon \geq 0$. In particular, we look at a neighbourhood of L_1 where complicated dynamics related to homoclinic tangencies are to be expected. As an example, we plot a few attractors for $\mathcal{P}_\varepsilon$ in Figures 5 and 6, for parameter values near the homoclinic curve L_1^a in region 9 of Figure 4. We have numerical evidence for

the following statements. Figure 5 shows a strange attractor that consists of 11 connected components mapped by $\mathcal{P}_\varepsilon$ to one another in a cyclic way. These components in Figure 6 'connect' in a scenario called heteroclinic tangency (or boundary crisis), compare [30]. A more systematic approach of this and related time-periodic systems is subject of future research.

Remark 2.2. When applying quasi-periodic forcing to system (2.3), local bifurcations in (2.3) give rise to quasi-periodic bifurcations [24, 23]. In the case of Hopf bifurcation, resonances are encountered between internal and forcing frequencies [75, 85]. See §3 and §5 for details on resonant dynamics.

3 Quasi-periodic Response Solutions at A Strong Resonance

Our second case originates from Stoker's problem [79], which asks for response solutions in quasi-periodically forced damped oscillators. To be definite, as a leading example we consider the forced Duffing – Van der Pol oscillator

$$\ddot{y} + \left(a + cy^2\right)\dot{y} + by + dy^3 = \varepsilon f(\omega_1 t, \ldots, \omega_m t, y, \dot{y}, a, b, c, d, \varepsilon).$$

Here the perturbation f is assumed to be periodic in its first m arguments with period 2π. This non-autonomous second order differential equation can be written as a vector field (in system form)

$$\left\{\begin{array}{rcl} \dot{x}_j &=& \omega_j, \qquad j = 1, \ldots, m, \\ \dot{y}_1 &=& y_2, \\ \dot{y}_2 &=& -\left(a + cy_1^2\right) y_2 - by_1 - dy_1^3 + \varepsilon f(x_1, \ldots, x_m, y_1, y_2, a, b, c, d, \varepsilon), \end{array}\right. \tag{3.1}$$

defined on the phase space ${}^m\times^2 = \{(x_1, \ldots, x_m), (y_1, y_2)\}$. Here ${}^m = {}^m/(2\pi^m)$ denotes the standard m-torus and $x = (x_1, \ldots, x_m) \in {}^m$ is called *internal* variable. Moreover, $y_1 = y$ and $y_2 = \dot{y}$ are called *normal* variables. To begin with, we may take f independent of (c, d), including only (a, b) as parameters. Accordingly, for the moment we abbreviate $\sigma = (a, b)$. However, we note that for later purposes and as an illustration of our main message we shall take (a, b, c, d) as parameters. Throughout we fix the frequency vector $\omega \in {}^m$, but in certain other cases ω may be included as an extra multi-parameter. Finally $\varepsilon \in$, with $|\varepsilon| \ll 1$, is a perturbation parameter. We assume f and all other functions to depend infinitely differentiably (or smoothly) on all their arguments.

Note that (3.1) is a skew system in the sense that the internal dynamics are independent of the normal variables. This allows one to focus on the influence of the internal dynamics on the normal dynamics, without having to take care of internal resonances. It is assumed that the frequencies $\omega_1, \ldots, \omega_m$ are rationally independent, in which case the forcing is called quasi-periodic.

The existence of a quasi-periodic response solution of frequency vector ω reduces to the existence of an invariant m-torus of (3.1) in the phase space ${}^m\times^2$, which is a graph $y = y(x)$ over ${}^m \times \{0\}$; each such m-torus corresponds to an m-parameter family of response solutions

$y = y(x(t))$. In the case of strong damping $|a| \gg 1$ (with a either positive or negative) the problem is solved in [79]: in a more contemporary language, it reduces to the persistence of normally hyperbolic invariant m-tori close to $^m \times \{0\} \subset^n \times^2$; the corresponding region in the parameter space often is called the 'Stoker domain'. The problem is more involved in the case of small damping $|a|$, as we shall discuss now. For details see [15, 24, 23, 41, 20, 75].

3.1 Quasi-periodic Hopf Bifurcation

In the case that $|a| \ll 1$ small divisors enter into the problem, as was already observed by Moser [68], which makes application of KAM theory necessary. This, among other things, involves *Diophantine conditions* on the frequency vector $\omega = (\omega_1, \ldots, \omega_m)$. Given positive constants τ and γ, these conditions require that

$$|k\omega - \ell\alpha(\sigma)| \geq \gamma |k|^{-\tau},$$

for all $k \in^m \setminus\{0\}$ and for $\ell = 0, 1, 2$. Here is the standard inner product and $|k| = \Sigma|k_j|$. Moreover $\alpha(\sigma) = \sqrt{4b - a^2}$ is the normal frequency, also see below. For $\tau > m - 1$ and $\gamma > 0$ small, the corresponding set of Diophantine frequency vectors has positive measure; for details see, e.g., [23, 24, 41]. Note that a Diophantine frequency vector surely has rationally independent components, which brings us in the above quasi-periodic set-up.

Generically this setting involves a Hopf bifurcation of the corresponding free oscillator. Fixing a Diophantine frequency vector ω, one needs at least two parameters to describe the phenomenon well; we first restrict to cases where we can take $\sigma = (a, b)$, for a near 0.

Normal-internal resonance. To explain what is going on, we generalize the above set-up by considering the family of vector fields

$$\begin{aligned} X_{\sigma,\varepsilon}(x, y) &= \omega + Z_{\sigma,\varepsilon}(x, y) \\ &= \omega + (A(\sigma)y + B(y, c, d) + \varepsilon F(x, y, \sigma, c, d, \varepsilon))\, y, \end{aligned} \tag{3.2}$$

where $(x, y) \in^m \times^2$, using the shorthand notation $\omega = \sum_{j=1}^m \omega_j \frac{\partial}{\partial x_j}$. Note that in the above example (3.1)

$$A(\sigma) = \begin{pmatrix} 0 & 1 \\ -b & -a \end{pmatrix}, \qquad B(y, c, d) = \begin{pmatrix} 0 \\ -cy_1^2 y_2 - dy_1^3 \end{pmatrix},$$

recalling that $\sigma = (a, b)$. Also we consider the vector field

$$N_\sigma(x, y) = \omega \frac{\partial}{\partial x} + A(\sigma) y \frac{\partial}{\partial y},$$

which is the normal linear part of the unperturbed invariant m-torus $^m \times \{0\} \subset^m \times^2$, see [24]. We note that N_σ is of Floquet form, i.e., independent of the internal variable $x \in^m$. Let $\mu(\sigma) \pm i\alpha(\sigma)$ denote the complex conjugate eigenvalues of $A(\sigma)$. In the Duffing – Van der Pol

example (3.1) we assume that $a^2 < 4b$, noting that $\mu(\sigma) = -a$ and $\alpha(\sigma) = \sqrt{4b - a^2}$. In general we call $\omega_1, \ldots, \omega_m$ the internal frequencies and α the normal frequency of the unperturbed m-torus.

A normal-internal $k : \ell$ resonance of $^m \times \{0\}$ occurs if

$$k\omega + \ell\alpha(\sigma) = 0, \tag{3.3}$$

for some $k \in^m$ and $\ell \in$ not both equal to zero. The smallest absolute value $|\ell|$, where ℓ ranges over all integers for which there is a $k \in^m$ such that (3.3) holds, is called the order of the resonance. Resonances of order up to 4 are called strong resonances [81, 5]; all other resonances are called weak. If for $\sigma = \sigma_0$ the torus $^m \times \{0\}$ is respectively non-resonant, weakly resonant or strongly resonant, the value σ_0 is called a non-degenerate, weakly resonant or strongly resonant quasi-periodic Hopf bifurcation value.

The weakly resonant case. The non-degenerate quasi-periodic Hopf bifurcation, as well as its weakly resonant analogue, have been investigated by Braaksma and Broer [15] for Diophantine internal frequency vectors ω. For small positive values of , system (3.2) has in its parameter space a codimension 1 submanifold $\mathcal{H}$, carrying a quasi-periodic Hopf bifurcation set $\mathcal{H}_c$ that has positive measure in $\mathcal{H}$. The set $\mathcal{H}_c$ is found by KAM theory. At every point $\sigma \in \mathcal{H}_c$, two open disk-shaped regions $\mathcal{A}_\sigma$ and $\mathcal{R}_\sigma$ exist in the complement of $\mathcal{H}$ and separated by $\mathcal{H}$ meet with infinite order of contact at $\mathcal{H}_c$. For parameter values in $\mathcal{A}_\sigma$, the vector field has an attracting normally hyperbolic m-dimensional invariant torus close to $^m \times \{0\}$; for values in $\mathcal{R}_\sigma$, a repelling one. Moreover, there are two possibilities regarding invariant $(m + 1)$-dimensional tori of (3.2). This distinction depends on the type (supercritical or subcritical) of the autonomous Hopf bifurcation as it occurs in the free oscillator given by (3.2) for $\varepsilon = 0$. Indeed, there exists a subset $\mathcal{H}_c^+ \subset \mathcal{H}_c$ of positive (relative) measure, such that for $\sigma \in \mathcal{H}_c^+$ there is another disk $\mathcal{A}_\sigma^+ \subset \mathcal{A}_\sigma$ in the supercritical case, or $\mathcal{R}_\sigma^+ \subset \mathcal{R}_\sigma$ in the subcritical case. In the first case, for parameter values in $\mathcal{A}_\sigma^+$ there exists an invariant attracting $(m+1)$-torus in the system; in the second case, there is an invariant repelling $(m + 1)$-torus for parameter values in $\mathcal{R}_\sigma^+$. All these invariant tori are of finite differentiability; the size of sets $\mathcal{A}_\sigma, \mathcal{A}_\sigma^+$ etc. shrinks if we impose a higher degree of differentiability. The disks $\mathcal{A}_\sigma^+$, $\mathcal{A}_\sigma$, $\mathcal{R}_\sigma^+$ and $\mathcal{R}_\sigma$ are all found by centre manifold theory. For more details see [15, 23, 24].

In the context of the Duffing – Van der Pol example (3.1), we sketch in Figure 7 the situation in the parameter space for the case where $\sigma = (a, b)$, so in a two-dimensional parameter space. At the present level the quasi-periodic Hopf bifurcation has codimension 2. Loosely speaking, μ serves as bifurcation parameter, while α keeps track of the normal frequency. For a discussion how a one-parameter Hopf-Landau family relates to a two-parameter quasi-periodic Hopf bifurcation, see [23]. Now we shall consider cases of strong normal-internal resonances, a proper discussion of which requires the availability of more parameters.

Remark 3.1.

1. Central for the above results is a quasi-periodic normalisation process [15, 24], also see below, which leads to a principal part based on the standard Hopf bifurcation for planar vector fields (and close to the one in the underlying free oscillator). After normalization and truncation a $^{m+1}$-symmetry can be factored out. Here the normal linear part $N = N_\sigma(x, y)$, for $\sigma \in \mathcal{H}_e$, plays a fundamental role. The (relative) equilibria then roughly correspond to m-tori and the periodic solutions to $(m+1)$-tori. For more details, generalisations and references see [15, 18, 24, 23, 41, 20, 57, 58].

2. We recall that in the periodic case $m = 1$ the boundary between the attracting and repelling m-tori (i.c., periodic solutions), away from the strong resonances, is smooth; this case is known by the names Hopf-Neĭmark-Sacker [52,63]. The weak resonances do play a role in the occurence of Arnold tongues [5, 80, 21] related to phase-lock dynamics on the normally hyperbolic 2-tori that branch off. In the present case $m \geq 2$ the boundary between the attracting and repelling m-tori is expected to become 'frayed' by the normal-internal resonances (3.3).

   It is to be noted that in [15,24,23] the resonance holes have a somewhat proof generated character. In [75, 87] the expectation of a 'frayed' (and non-smooth) boundary is given further ground by showing the existence of resonant dynamics.

3.2 Normal-internal Resonance: Setting of the Problem

We are interested in the complement of the parameter domains with normally hyperbolic invariant m- and $(m+1)$-tori. This complement consists of countably many resonance holes (or bubbles) related to the normal-internal resonances (3.3), in particular for the cases with $\ell \geq 3$. Compare with Figure 7. For persistent case studies in the context of a quasi-periodic saddle-node bifurcation, see Chenciner [38, 39, 40].

We extend the research initiated by Gambaudo [45] and Wagener [87] on the strong resonances with $\ell = 1, 2$, both for the cases $m = 1$ and $m = 2$, compare with [75]. After appropriate averaging [19, 16, 77] and truncation, in [45, 87] a ^{m}-symmetry can be divided out and a bifurcation analysis of the resulting principal part is held, centered around the (relative) equilibria. The corresponding 'local' bifurcations have been tracked down, and also certain 'semi-global' phenomena occur in the analysis. This is exactly what makes the example fit in the present discussion.

To be precise, for the cases $\ell = 1$ and $\ell = 2$, the bifurcation diagrams are completed. For the former case, the bifurcation diagram of the principal part is understood completely by taking the codimension 3 singularity of nilpotent-elliptic type [43], found in [87] as organising centre. As a direct consequence, we also find a codimension 2 degenerate Hopf bifurcation, which was still absent from [45, 87]. For both the cases $\ell = 1, 2$ we add curves of homoclinic and heteroclinic global bifurcations to the bifurcation diagram, with help of AUTO [42] and Matlab [53].

The first step in the analysis of the quasi-periodic case amounts to understanding the periodic case. Though these two scenario's are strongly related the quasi-periodic case is more

involved than the periodic one. The fact that the resonating normal frequencies are dense in the set of all normal frequencies implies that the overall quasi-periodic picture has a lot more fine-structure.

3.3 Further Background

For a systematic bifurcation analysis of the periodic resonances see Takens [81]. There, with help of normal form theory the generic strong ($1:\ell$ for $\ell = 1,\ldots,4$) and weak ($\ell \geq 5$) resonances of periodic response solutions were studied by their Poincaré mappings and a corresponding vector field principal parts. For the $1:4$ resonance see [59, 60].

In this respect, the $1:1$ resonance, also see [5, 6, 13, 14], gives rise to the Bogdanov-Takens bifurcation. However, from a practical point of view, the Bogdanov-Takens bifurcation does not fully describe what happens generically to the response solutions of a driven damped oscillator at resonance. Indeed, for certain parameter values, there are two response solutions, while for others there are none. However under natural hypotheses, like e.g. the friction coefficient growing sufficiently quickly with amplitude, a topological argument can be employed to show the existence of at least one response solution in the oscillator [37]. With help of index theory it is shown that at least one equilibrium exists in the oscillator dynamics.

This implies that simultaneously to the response solutions related to the Bogdanov-Takens bifurcation, there is yet another response solution, which, for parameter values close to the Bogdanov-Takens bifurcation value, is 'far away' and thus is not captured by a local analysis. Holmes and Rand [56, 52] gave a semi-global analysis of the $1:1$ resonance in a special case where all response solutions are captured. The term 'semi-global' here means that after averaging and scaling, we consider phenomena in a given 'large' region of the phase space, rather than in the infinitesimally small regions related for purely local bifurcation analysis. Compare with, e.g., [87, 62, 70, 61].

The analysis of Holmes and Rand was extended by Gambaudo [45] to a semi-global bifurcation analysis of the generic codimension 2 cases of strong resonances. Note that recently a beginning has been made of analysing resonances of periodic response solutions at degenerate resonant bifurcations [21]. In that case resonances $1:\ell$ are strong if $\ell \leq 6$ and weak otherwise. As we find families of degenerate Hopf bifurcations in our analysis, the phenomena reported in [21] will probably occur in our system as well.

3.4 Sketch of Results

In [87] Wagener has taken up the semi-global analysis of driven damped anharmonic oscillators at resonant bifurcation in case that the driving is quasi-periodic instead of periodic, see the set-up (3.2). In this context, the $1:1$ resonance gives rise to quasi-periodic Bogdanov-Takens bifurcation. As mentioned before, in the first step of such an investigation normalising or averaging techniques are applied [6, 80, 35, 36, 19, 60], that permit to write the system as a periodically forced system with a small quasi-periodic perturbation term. Working in a different

parametrisation from [56, 52, 45], and considering a third natural parameter, analysis of the periodic part yields that in the $1:1$ resonance, the two generic cases reported in [45] can be seen as subfamilies of a generic three-dimensional bifurcation diagram that is organised by a singularity of nilpotent-elliptic type (see [43]).

The analysis initiated in [87] is completed in [75], also see [76], by taking the singularity of nilpotent-elliptic type as organising centre of the bifurcation diagram and exploring the implications of this. In this way, the occurrence of degenerate Hopf bifurcations in the $1:1$ resonance case is shown. We compute all global bifurcation curves that are known from the analysis of the singularity of nilpotent-elliptic type, except those relating to 'boundary bifurcations'. The latter concerns tangencies of the vector field to the boundary of any small neighbourhood containing the singularity [44]. Note that this concept is not related to the transcritical bifurcation. Further, a complete two-dimensional bifurcation diagram for the case $1:2$ resonance is given, also see [61, 62, 70, 45, 84]. In the quasi-periodic context, this gives rise to quasi-periodic $1:2$ resonant bifurcation.

Moreover, the differences between periodicity and quasi-periodicity are spelled out more fully. For instance, as said before, in the periodic case the Hopf bifurcation set is a smooth manifold. In the quasi-periodic case, it is shown in [87] that every resonance between the perturbing quasi-periodic frequency ω and the Floquet exponent α of the free oscillator generically gives rise to a resonance hole. This gives further ground to the expectation that the Hopf bifurcation set is frayed. We shall invoke quasi-periodic bifurcation theory [38, 24, 91] to investigate which portions of the local bifurcation diagram persist under small perturbations. In the bifurcation diagram there are quasi-periodic Hopf bifurcation sets for which the present analysis can be applied repeatedly: in this way resonance within resonances are found, as in, e.g., [9]. For a Hamiltonian analogue of the present program see [22].

Resonant normal forms. Let $k\omega + \ell\alpha_0 = 0$ for either $\ell = 1$ or $\ell = 2$. For λ close to $i\alpha_0$, performing successive 'normal form' or 'averaging' transformations [19, 16, 36, 22] and scaling of phase phase and parameter space, yields a coordinate system relative to which the vector field X is of the form

$$X = \omega x + \delta^2\, \Re\Big(\lambda z + {}^{i\theta}\,|z|^2 z + \bar{z}^{\ell-1}\Big)\, z + \delta^3 \tilde{Z}\ .$$

See [75] for details. We put

$$Z_0 = \Re(\lambda z + {}^{i\theta}\,|z|^2 z + \bar{z}^{\ell-1}) z\ . \tag{3.4}$$

From the more precise results derived in [76, 29] it follows that X can actually be put in the form

$$X = \omega x + \delta^2 \left(Z_0 + \delta Z_1 + \delta^N Z_2\right), \tag{3.5}$$

where Z_1 is an integrable vector field, and where N can be choosen arbitrarily large. The present semi-global context motivates the study of this equation for $\ell = 1$ and $\ell = 2$.

Bifurcation analysis of the $k:1$ resonance. Now we perform a bifurcation analysis of the vector field Z_0, see (3.4), for the case $\ell = 1$. The analysis is complete with respect to local bifurcations, which are obtained analytically. Using numerical tools like Matlab [51, 53] and AUTO [42], we detect global bifurcations, i.e., homoclinic loops and saddle-node bifurcations of limit cycles.
Consider the principal part

$$Z_0 = \Re\left(\lambda z + ^{i\theta}|z|^2 z + 1\right) z\ . \tag{3.6}$$

We shall see that the bifurcation diagram of this family has a codimension 3 singularity of nilpotent-elliptic type as organising centre 'outside this family'. Observe that Z_0 is symmetric with respect to the group generated by the involutions

$$(t, z, \lambda, \theta) \mapsto (t, \bar{z}, \bar{\lambda}, -\theta) \qquad \text{and} \qquad (t, z, \lambda, \theta) \mapsto (-t, -z, -\lambda, \theta + \pi).$$

Because of this symmetry, we can restrict our attention to the part of parameter space for which $0 \leq \theta \leq \pi/2$.

Figure 8 gives a graphical overview of our results on the position of the bifurcation manifolds that correspond to local bifurcations of codimension 1 and 2. The codimension 2 bifurcation curves corresponding to cusp and Bogdanov-Takens bifurcations are indicated in Figure 8(a). Figure 8(b) shows the relative positions of the codimension 1 bifurcation manifolds in the vicinity of a NE_3 point.

We extend the description of the bifurcation diagram of equation (3.6) given in [87]. In Figure 9, we plot all singularities of system (3.6) for the two-dimensional section $\mathcal{S}_2$ of Figure 8(a), as well as the generic phase portraits of the system for parameters in different regions of the bifurcation diagram. For the two-dimensional section $\mathcal{S}_1$ see [76, 75].

We find all local bifurcations of (3.6): saddle-node (SN_1), Hopf (H_1), cusp (SN_2), Bogdanov-Takens (BT_2) and degenerate Hopf (H_2) bifurcations, which are expected from the bifurcation diagram of a singularity of nilpotent-elliptic type [44]. We also retrieve homoclinic (L_1) and saddle-node of limit cycles bifurcations ($SNLC_1$); these are found using the numerical packages AUTO [42] and Matlab [53, 51] respectively.

Remark 3.2. System (3.6) also contains a global feature, namely, a large homoclinic loop of a hyperbolic saddle-point, which is not explained by the NE_3 point. This large homoclinic loop is detected by AUTO [42]. See Figure 9.

Bifurcation analysis of the $k:2$ resonance. As in our previous investigation, here we perform a bifurcation analysis of the vector field Z_0, see (3.4), for the case $\ell = 2$. As remarked before, in this case it is sufficient to consider two bifurcation parameters. The local bifurcations in the $\ell = 2$ case have already been given in [45, 87]; in this section, after briefly recalling those results, global bifurcations are determined numerically whose existence follows from our knowledge of the local bifurcation diagram.

Consider the principal part

$$Z_0 = \Re\left(\lambda z + {}^{i\theta}\,|z|^2 z + \bar{z}\right) z\ . \tag{3.7}$$

As before, this is a two-parameter family of planar vector fields (parameterised by $\lambda \in \mathbb{C}$) as we shall treat θ as a generic constant. Observe that Z_0 is symmetric with respect to the group generated by the two involutions

$$(z, \lambda, \theta) \mapsto (\bar{z}, \bar{\lambda}, -\theta) \qquad \text{and} \qquad (z, \lambda, \theta) \mapsto (-z, \lambda, \theta).$$

Because of this symmetry, we restrict our attention to those values of θ satisfying $0 \leq \theta \leq \pi$.

The bifurcation diagram of (3.7) is depicted in Figure 10. From the occurrence of a Bogdanov-Takens bifurcation, we infer the existence of a homoclinic bifurcation curve L_1. One symmetric double zero SDZ_2 bifurcation gives rise to curves of saddle-nodes of limit cycles $SNLC_1$, Hopf bifurcations H_1 and homoclinic loops L_1. This last curve ends on the curve of pitchfork bifurcation PF_1; at that point, a curve of heteroclinic bifurcation points HE_1 departs that ends on a line of saddle-nodes of equilibria SN_1. At the other SDZ_2 point, we have a second curve of heteroclinic bifurcations HE_1, also ending on a saddle-node line.

For $\ell \geq 3$ techniques from KAM theory (see [16]) can be applied to show the existence of invariant tori close to $\mathbb{T}^m \times \{0\}$, also compare with [31, 32, 24].

4 Related Settings

The approaches in §3 and §4 both fit into a larger frame of related research, including many applications. For details we refer to [29, 75] and their bibliographies. In this section we present a few further illustrations of the organising centre principle, though we do not attempt to be complete.

4.1 Meteorological Dynamics

The Lorenz84 climate model [64] is a three-dimensional vector field depending on four 'physical' parameters a, b, F and G. The model is obtained from the so-called 'primitive equations' (which are Navier-Stokes based) of the atmosphere by a procedure involving a Galerkin projection, *i.e.*, truncation to low modes of a Fourier expansion of the solution, see [83]. Regarding the numbers of degrees-of-freedom and of control parameters the Lorenz84 system is the simplest model describing atmosphere dynamics at midlatitudes of the northern hemisphere. Due to the severe truncation, however, the model is not suitable for quantitative predictions or statistical studies. Its main climatological appeal lies in the simple representation of a dominant physical process in the atmosphere, namely the interaction between westerly jet stream and baroclinic waves.

In [78] a bifurcation analysis is given of a principal part vector field, in dependence of the two parameters F, G; in most research on the subject a and b are kept constant. This analysis forms the basis of many ensuing studies on Lorenz84. For the present purposes we just

mention [31,32,83,85]; referring for further reading to their extensive bibliographies. In [83], the effect on the (F,G) bifurcation diagram of varying a third parameter b is studied. Next, in [31,85] the parameters (F,G) are made periodic in a perturbative way, thereby modelling seasonal effects. This amounts to a three-dimensional Poincaré return map analysis, depending on three parameters.

In all these cases, it turns out that quite a few local codimension 2 bifurcations act as organising centers, among which a Hopf saddle-node (HSN) bifurcation [52, 63] as well as several strong resonances [5, 81]. Moreover, behind the semi-global array of bifurcations a few singularities of higher codimension act as organising centers; among those are certain degenerate Bogdanov-Takens and Hopf bifurcations [43] and degenerate versions of the HSN bifurcation. Many of the latter have not yet been studied theoretically and certain models are recently being investigated [34]. It should be mentioned that in the HSN model for maps, in the analysis of a normal-internal resonance, once more underlying degenerate Bogdanov-Takens and Hopf bifurcations act as organising centers. Compare with §4 above and with, e.g., [75]. For a theoretical link of the climate models with chaos see [32, 33].

4.2 Economic Dynamics

The Brock-Hommes [17] model for price dynamics of risky assets sketches a simplified picture of a stock market. There are many agents on this market, who can invest in either a risky asset (a stock) or a riskless asset (e.g. a bond). All prices are expressed in units of the riskless asset, which pays a known fixed interest each period. The risky asset pays a random dividend; moreover, the market price of this asset in the next period is unknown and therefore subject to speculation.

Though there are many traders, in the simplest set-up it is assumed that their beliefs (or predictions) on the next-period price of the risky asset is of either of two types: there is the fundamental belief, which holds that the 'true' or 'fundamental' value of the risky asset is equal to the discounted stream of future dividends, and which therefore expects that the next-period price will be closer to the fundamental value than the current price. The other group of traders is more pragmatic and expects, for example, that the next-period price can be predicted by some linear extrapolation of recent prices. This prediction method is called 'trend-chasing' or 'technical analysis', as it mimics the kind of price chart analysis which is actually performed by stock traders. Every period, a trader decides on the prediction rule to be used to determine his demand for the risky asset on the basis of the past success of the two rules.

In a recent set of papers [47, 46], a variant of this model has been subjected to bifurcation analysis, where three parameters were considered: the switching rate β ('intensity of choice'), which determines how precisely the traders perceive which strategy is the better of the two; the adaptation rate v of the fundamentalist belief, determining the speed at which the price is assumed to converge to the fundamental price; and the trend parameter g, which controls the price change that trend chasers expect from the recent price data.

Keeping first the parameters v and β at some 'typical' values, the following bifurcation scenario is observed: for values of the trend parameter g smaller than 1, the fundamental steady state is stable, and both fundamentalists and trend chasers make the same predictions: the market is homogeneous. Then, as g increases, a pair of invariant circles are generated in a saddle-node bifurcation far away from the fundamental state. The unstable circle then shrinks in size until it vanishes in a subcritical Hopf bifurcation involving the fundamental steady state.

The economic interest of this scenario is the following: the deterministic dynamical system is seen as an approximation to a stochastic situation, where for instance the supply of the risky asset on the market is taken as a random quantity. Consider now parameter values such that there are a stable fundamental steady state and a stable invariant circle in the system, each having a basin of attraction. The stochastic dynamics follow the deterministic dynamics most of the time, but if the shocks are great enough, the system can jump from one basin of attraction to the other. These jumps will by necessity be uncorrelated in time. It follows that the resulting market will have 'quiet' periods, for which the price is close to the fundamental, and 'lively' periods, for which the price is tracking the dynamics on the invariant circle.

The two bifurcations, saddle-node of invariant circles and subcritical Hopf bifurcation of the fundamental steady state, seem to be unrelated in a one-parameter bifurcation study. But they are seen to be connected when the system is studied with three parameters, for there is a curve of degenerate Hopf bifurcations (H_2 in Table 1.1) acting as organising centres of this system.

4.3 Dynamic Optimisation

In a typical dynamic optimisation problem an evolution law of a system variable is given, for instance the amount of capital available to a firm, the stock of pollutant in a lake or the position of a ship with respect to the harbour. It is assumed that this evolution can be influenced by exercising a control, like investing in capital in the first example, reducing pollution in the second and changing speed or direction of the course of the ship in the last example. The object of controlling the system is either to minimise some total cost or to maximise some total benefit derived from the system. There is always a trade-off between several conflicting interests at work. For instance, the manager of the firm tries to reach high production and high profits through an accumulation of firm capital, but investment is costly; the local government dealing with the lake has to weigh the interests of the farmers, whose use of artificial fertiliser pollutes the lake, against those of tourists and water companies, who prefer very much a clean lake. Finally, the ship's captain tries to reach the harbour quickly, but without using too much fuel.

The optimal choice for the control is obtained from the solution of a certain dynamical system, the state-costate system, that has twice as many variables as the dimension of the system's state. For the economic applications that we are interested in, this system is a perturbation of an autonomous Hamiltonian system, where the perturbation term is related to the amount of discounting of future costs relative to present costs. In this case, the autonomous system acts as a principal part.

Pollution of a lake. In the lake system as investigated in [89], there are three basic parameters: the sedimentation rate b, which determines the speed at which the pollutant moves from the water in the lake to the sediment at the lake's bottom; the economic parameter c, which determines the relative weight of the tourists' interest relative to those of the farmers; and the discount rate ρ described above.

As the sedimentation rate is a physical characteristic of the lake, in a first analysis this is kept fixed. Also the discount rate is fixed, giving us a one-dimensional 'slice' or 'probe' of the three-dimensional parameter space. For typical values of b and ρ, there are then three different solution structures: for low values of c, it is always optimal to let the lake serve as a waste dump, leading to a steady state of the lake where it is highly polluted. For high values of c, it is likewise always optimal to restrict severely the use of fertiliser on the farmland surrounding the lake, such that the lake can reach a clean steady state at which there is but little pollutant in the lake. Finally, for intermediate values of c, one of the two options described is optimal, but now this depends on the initial state of the lake.

It turns out that the separate regions are bounded by two codimension one heteroclinic bifurcations of the state-costate system. If we now consider the system in the full three-dimensional parameter space, the corresponding heteroclinic bifurcation surfaces end on two saddle-node surfaces of equilibria of the state-costate system, that in turn meet in a curve of cusp bifurcations. All these bifurcation curves are finally seen to originate in a Hamiltonian cusp bifurcation, which, in this special set-up, is a codimension three organising centre. Note that the situation here is different from a 'generic' dynamical system, where a Hamiltonian bifurcation would be of infinite codimension; the difference is due to the special structure of economic optimisation problems.

Optimal investment. The optimal investment problem of a monopolistic firm investigated in [90] is analysed similarly. Here there are four parameters; the discount rate ρ and three more parameters that model the 'firm structure', that is the structure of the firm's costs and revenues. There are now three different possible steady states, corresponding to a firm of small, medium and large size, which may be reached by optimal investment schedules. The structure of the bifurcation diagram that summarises which firm size will be obtained optimally is suitably complicated, but it is as in the Lake Pollution problem organised by a single bifurcation, in this case a Hamiltonian swallowtail that has codimension 4 in the set-up of an economic optimisation problem. From the codimension 4 point, there is a curve of 'ordinary' codimension 3 swallowtail catastrophes projecting into our three-dimensional space of parameters. See Figure 1.1 for the ordinary swallowtail catastrophe.

5 Concluding Remarks

We briefly summarize the program of this research, which mainly sits within the 'general dissipative' setting without preservation of structure. In other cases (Hamiltonian, volume preserving, reversible, equivariant) the program has to be adapted, e.g., compare [22, 20].

A general and widely used approach to dynamical systems is the following, as reflected in the textbooks [52, 5]; also compare with, e.g., [92, 6, 19, 35, 49, 50, 77, 81, 80, 59, 60, 87].

The first step is to identify and analyse a relevant principal part of the system, obtained by projections and truncations of the Taylor-Fourier series and in such a way that the original system can be viewed as a perturbation of this principal part. Next, in the dissipative context, the attention goes to the structurally stable or Morse-Smale 'strata' and a corresponding bifurcation analysis, beginning with the principal part.

Our main message is that the analysis of the principal part often benefits from considering more parameters. Certain semi-global arrays of bifurcations turn out to be subordinate to one or more bifurcations of higher codimension.

Next, conclusions from the principal part analysis to bifurcations of the original systems run by perturbation theory, often containing an application of Singularity Theory and an underlying universal problem.

A second message then is how this bifurcation analysis of the principal part gets complicated when periodic and quasi-periodic perturbations are applied. This complication and fine-structuring is due to resonances and, generically, the effects on the bifurcation diagrams can be well-described, [15, 24, 23, 20, 18, 22, 38, 39, 40, 54, 88, 75]. We note that by the information thus obtained, it is often possible to identify parameter regions where chaos might be found, compare with §3.2 and, e.g., [29, 32, 33].

Acknowledgment

The authors like to thank Odo Diekmann, Bernd Krauskopf, Kurt Lust, Jean-Christophe Poggiale, Carles Simó, Floris Takens and Renato Vitolo for helpful discussion.

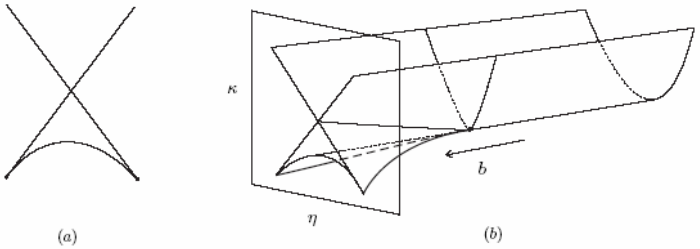

Figure 1: (a): Two-dimensional diagram with semi-global array of cusps and folds. (b): Three-dimensional diagram with swallowtail as organising centre.

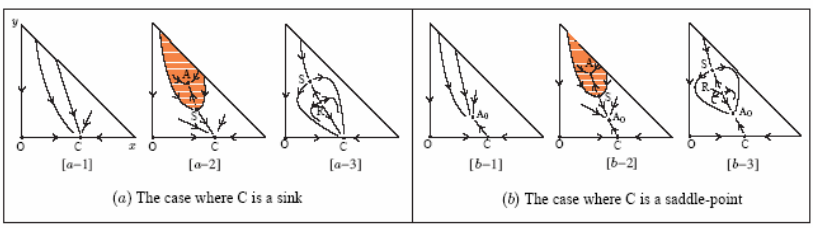

Figure 2: Reduced Morse-Smale portraits occurring in system (2.3); A is a sink (the corresponding basin is dashed), S is a saddle-point and R a source. (a): The case where C is a sink (with corresponding basin in white). (b): The case where C is a saddle-point. In the latter case the interior of the trapping domain always contains an attractor denoted by A_0 with basin in white. Bi-stability only occurs in portraits [a-2] and [b-2].

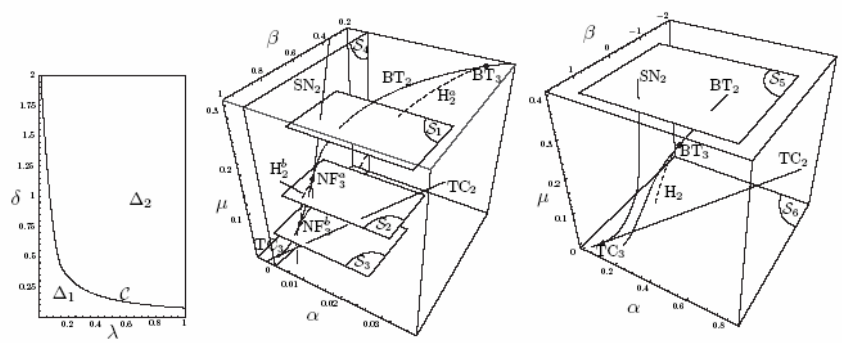

Figure 3: (a): Region $\Delta = \{\delta > 0, \lambda > 0\}$. (b): Bifurcation set in $\mathcal{W} = \{\alpha \geq 0, \beta > -2\sqrt{\alpha}, \mu \geq 0\}$ when $(\delta, \lambda) \in \Delta_1$. Section $\mathcal{S}_4 = \{\alpha = 0\}$ is the two-dimensional section associated to the bifurcation diagram of Bazykin's model [63]. (c): Similar to (b) for the case $(\delta, \lambda) \in \Delta_2$. Section $\mathcal{S}_6 = \{\mu = 0\}$ covers the case of Zhu's model [95]. For terminology see Table 1.

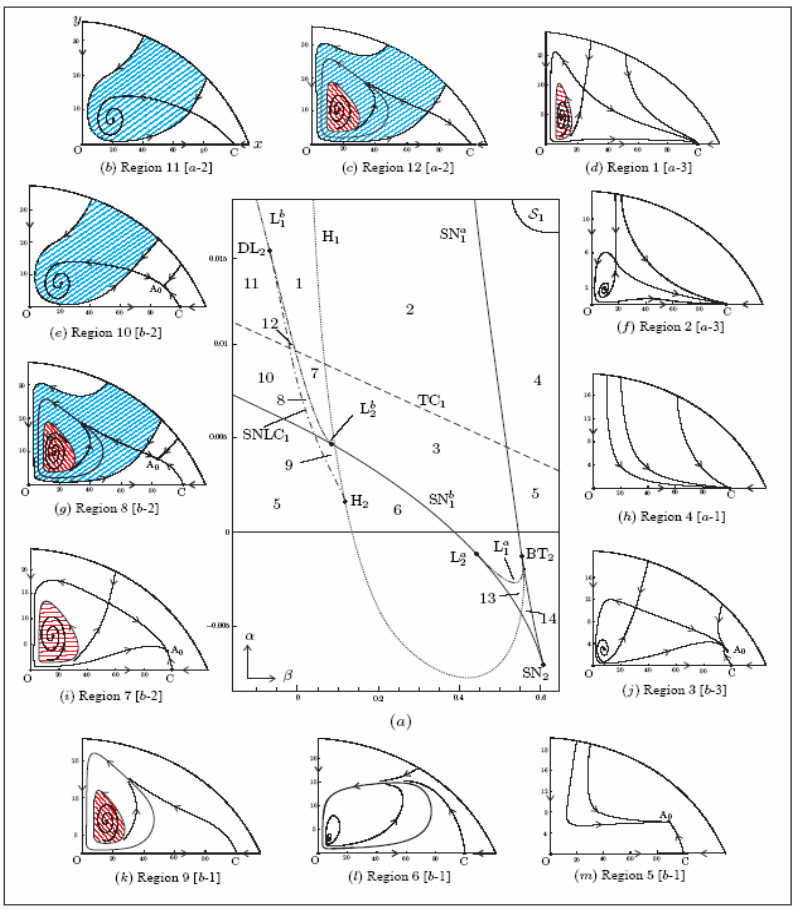

Figure 4: (*a*): Bifurcation diagram in two-dimensional section $\mathcal{S}_1 \subset \{\mu = 0.1\}$ of Figure 3-(b), $(\delta, \lambda) = (1.01, 0.01) \in \Delta_1$. A codimension 2 transcritical point lies on the curve TC_1 but is not mentioned since it occurs for $\beta \ll -\sqrt{\alpha}$. Note the presence of a cusp point (SN_2) and a Bogdanov-Takens point (BT_2) below $\{\alpha = 0\}$ both acting as organising centres. These points are depicted for a better understanding of the bifurcation set. (*b*)-(*m*): Associated phase portraits referring to the corresponding Reduced Morse-Smale portraits of Figure 2. Bi-stability in regions 8 and 9 both correspond to [*b*-2] in Figure 2. Bi-stability also holds in region 10 (corresponding to [*b*-1], which does not show bi-stability). The white basin of attraction is either for C or for A_0, while the shaded ones are for other attractors. For terminology see Table 1.

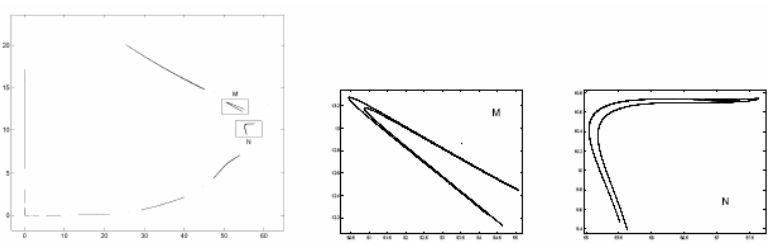

Figure 5: Left: Strange attractor for $\mathcal{P}_\varepsilon$ for parameter values in region 9 of Figure 4 using 500 000 iterations, $(\alpha, \beta, \mu, \delta, \lambda) = (0.007, 0.036, 0.1, 1.01, 0.01)$, $w = 1$ and $\varepsilon = 0.6$. The attractor consists of 11 connected components mapped by P_ε to one another in a cyclic way. Middle and Right: Magnifications of boxes M and N in the figure on the left.

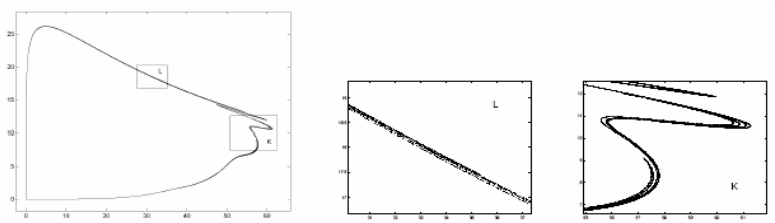

Figure 6: Left: Viana-like strange attractor for $\mathcal{P}_\varepsilon$ for parameter values in region 9 of Figure 4 using 500 000 iterations, $(\alpha, \beta, \mu, \delta, \lambda) = (0.007, 0.036, 0.1, 1.01, 0.01)$, $w = 1$ and $\varepsilon = 0.99$, compare [30]. Middle and Right: Magnifications of boxes L and K in the figure on the left, respectively.

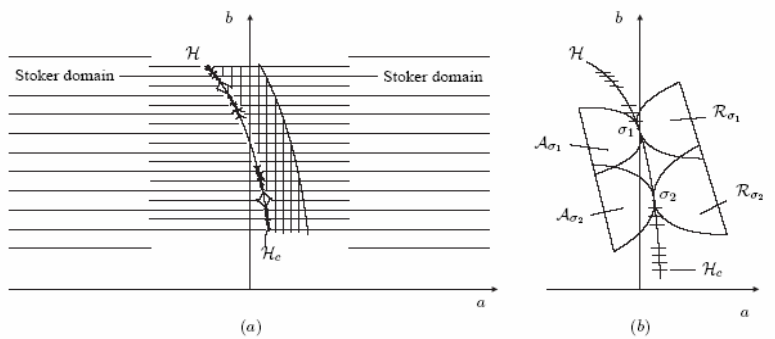

Figure 7: (a): Sketch of global bifurcation set $\mathcal{H}_c \subset \mathcal{H}$ of the quasi-periodic Hopf bifurcation in the context of the Duffing – Van der Pol example (3.1) with Stoker m-tori (shaded) and $(m+1)$-tori (doubly shaded) using $\sigma = (a, b)$, compare with [15]. (b): Detail with resonance hole or bubble between discs $\mathcal{A}_\sigma$ and $\mathcal{R}_\sigma$ attached to different $\sigma \in \mathcal{H}_c$.

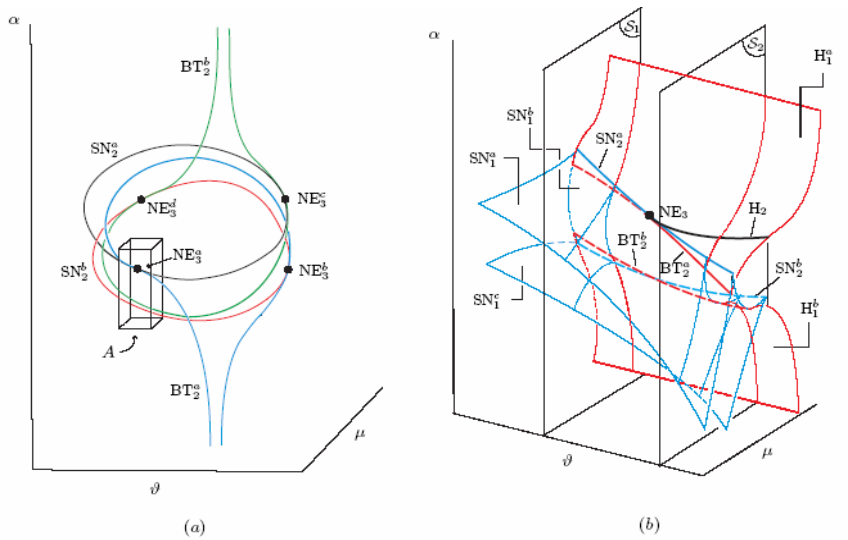

Figure 8: (a): Sketch of the global bifurcation diagram of $\dot{z} = (\mu + i\alpha)z + e^{i\vartheta}|z|^2 z + 1$ in the (ϑ, μ, α)-parameter space. All singularity of nilpotent-elliptic points (NE_3) are connected by cusp (SN_2) and Bogdanov-Takens (BT_2) lines. The curves BT_2^a and BT_2^b tend to $\pm\infty$, respectively, when ϑ goes to $\pi/2$. (b): Detail of the bifurcation set in box A of figure (a). At the singularity of nilpotent-elliptic type (NE_3) point, curves of Bogdanov-Takens (BT_2^a), cusp (SN_2^a), and degenerate Hopf (H_2) bifurcations meet tangentially. The curves BT_2^b and SN_2^b do not intersect. For terminology see Table 1.

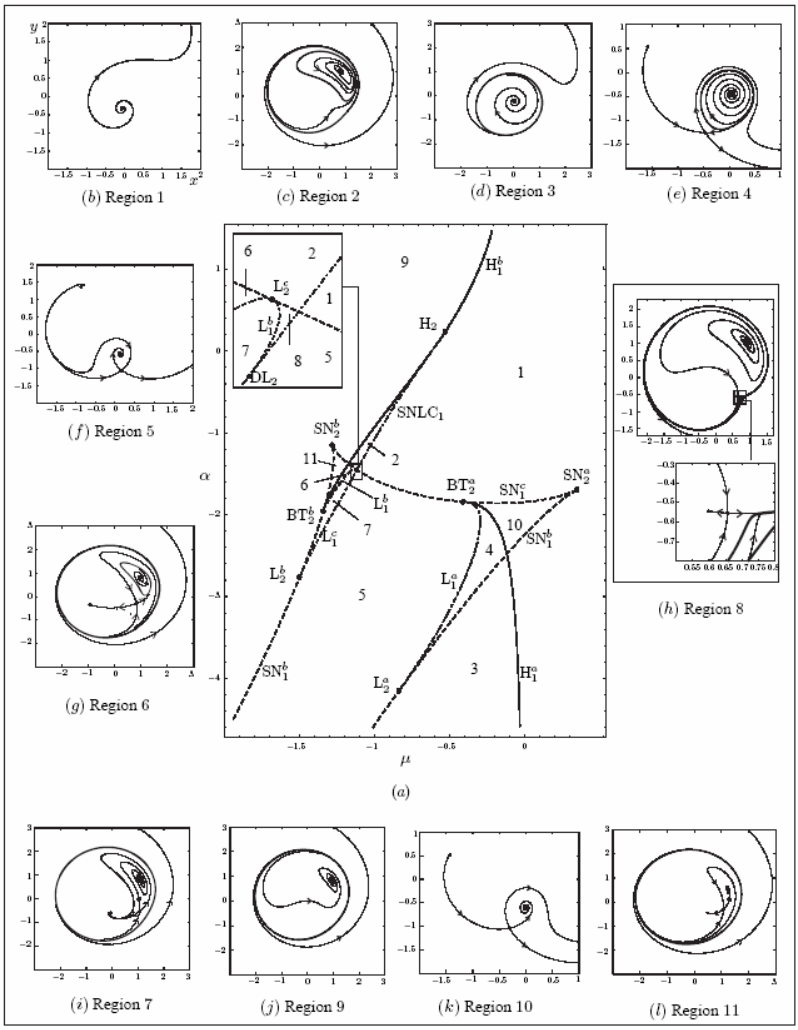

Figure 9: (*a*): Bifurcation diagram of (3.6) for $\vartheta = 2\pi/5$. (*b*)-(*l*): Phase portraits for parameters in the different regions of the bifurcation diagram of the family (3.6). For regions 1, 2, 3 and 9, single orbits, leaving an unstable equilibrium or unstable periodic orbits are shown. For all other regions, stable and unstable manifolds of saddle points are drawn. For terminology see Table 1.

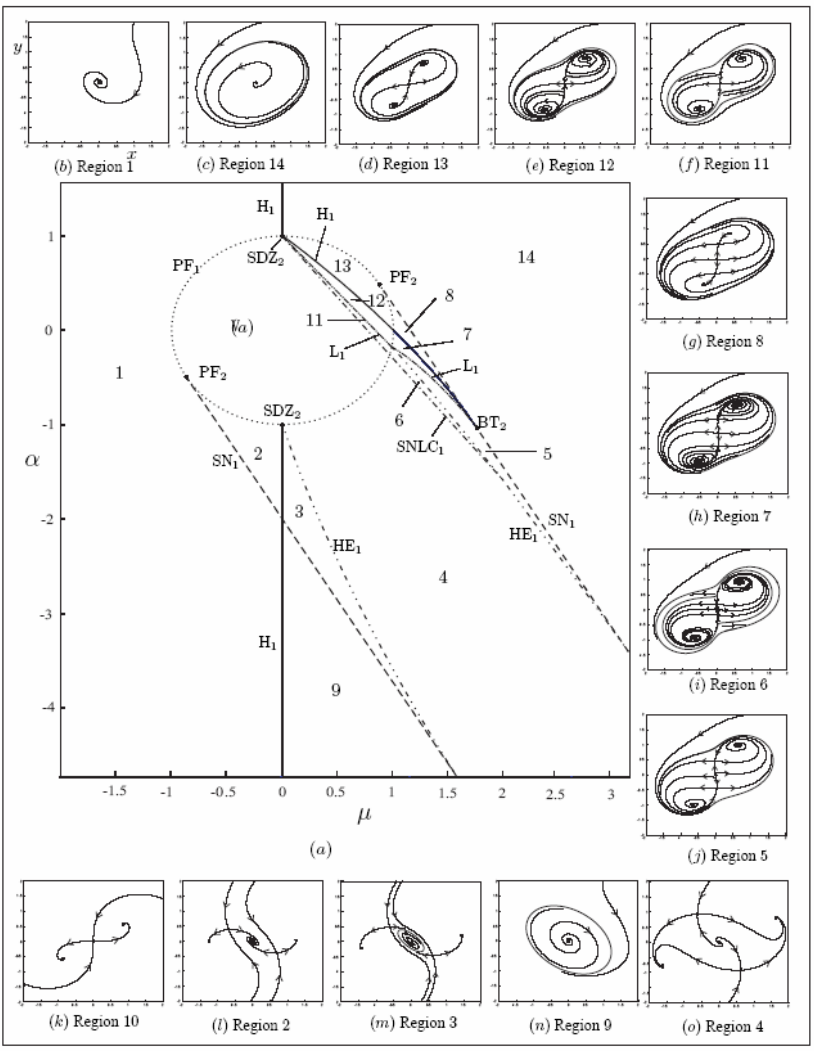

Figure 10: (a): Bifurcation diagram of $\dot{z} = (\lambda_1 + i\lambda_2)z + e^{i\vartheta}|z|^2 z + \bar{z}$ for $\vartheta = 2\pi/3$, compare with [45, 61, 62, 70, 84]. $(b) - (o)$: Generic phase portraits for different regions in the parameter space. For terminology see Table 1.

References

[1] Abraham, R. and Marsden, J. E. 1978. *Foundations of Mechanics*, Benjamin Cummings.

[2] Andrews, J. F. 1968. A mathematical model for the continuous of microorganisms utilizing inhibitory substatrates, *Biotechnol. Boieng.* **10**: 707–723.

[3] Arditi, R. and Ginzburg, L. R. 1989. Coupling predator-prey dynamics: ratio-dependence, *Journ. of Theo. Biol.* **139**: 311–326.

[4] Arnol'd, V. I. 1980. *Mathematical Methods of Classical Mechanics*, Springer-Ver.GTM **60**.

[5] Arnol'd, V. I. 1983. *Geometrical Methods in the Theory of Ordinary Differential equations*, Springer-Verlag.

[6] Arnol'd, V. I. 1989. Bifurcations and singularities in mathematics and mechanics. In: *Theoretical and Applied Mechanics XVII IUTAM*, Congress, Grenoble, 1988, Elsevier: 1–25.

[7] Arnol'd, V. I. 1992. *Catastrophe Theory*, Springer-Verlag.

[8] Arnol'd, V. I. (ed.) 1994. *Dynamical Systems V*, Encyclopædia of Mathematical Sciences **5**, Springer-Verlag.

[9] Baesens, C., Guckenheimer, J., Kim, S. and MacKay, R. 1991. Simple Resonance Regions of Torus Diffeomorphisms, Patterns and Dynamics of Reactive Media (Aris, Aronson and Swinney eds.), *IMA Volumes in Mathematics and its Applications* **37**: 1–11.

[10] Bazykin, A. D. 1998. Nonlinear dynamics of interacting populations, edited by A.I. Khibnik and B. Krauskopf, *World scientific series on nonlinear science* A **11**, World scientific.

[11] Bazykin, A. D., Berezovskaya, F. S., Denisov, G. and Kuznetsov, Y. A. 1981. The influence of predator saturation effect and competition among predators on predator-prey system dynamics, *Ecol. Modelling* **14**: 39–57.

[12] Beddington, J. R. 1975. Mutual interference between parasites or predators and its effect on searching efficiency, *Journ. of Animal Eco.* **44**: 331–340.

[13] Bogdanov, R. I. 1976. Bifurcations of a limit cycle of a family of vector fields in the plane, *Trudy Seminara Imeni I.G. Petrovskogo* **2** :23–36, Translation of: *Selecta Math. Sovietica* **1** (1981), 373–388.

[14] Bogdanov, R. I. 1976. A versal deformation of a singular point of a vector field in the plane in the case of vanishing eigenvalues, *Trudy Seminara Imeni I.G. Petrovskogo* **2**: 37–65, Translation of: *Selecta Math. Sovietica* **1** (1981), 389–421.

[15] Braaksma, B. L. J., and Broer, H. W. 1987. On a quasi-periodic Hopf bifurcation, *Annales de l'institut Henri Poincaré-Analyse nonlinéaire* 4: 115–168.

[16] Braaksma, B. L. J., Broer, H. W. and Huitema, G.B. 1990. Towards a quasi-periodic bifurcation theory, *Mem. AMS* **83**: 83–175.

[17] Brock, W. A. and Hommes, C. H. 1998. Heterogeneous beliefs and routes to chaos in a simple asset pricing model, *Journal of Economic Dynamics and Control* **22**: 1235–1274.

[18] Broer, H. W. 1989. Quasi-periodic bifurcations, applications *Proc. XI C.E.D.Y.A. (Málaga)* Universidad de Málaga: 3–22.

[19] Broer, H. W. 1993. Notes on Perturbation Theory 1991, Erasmus ICP *Mathematics and Fundamental Applications*, Aristotle University Thessaloniki: 44 p.

[20] Broer, H. W. 2004. KAM theory: the legacy of Kolmogorov's 1954 paper, *Bull. AMS* (New Series), **41**(4): 507-521.

[21] Broer, H. W., Golubitsky, M. and Vegter, G. 2003. The geometry of resonance tongues: a singularity theory approach, *Nonlinearity* **16**: 1511–1538.

[22] Broer, H. W., Hanßmann, H., Jorba, À., Villanueva, J. and Wagener, F. O. O. 2003. Normal-internal resonances in quasi-periodically forced oscillators: a conservative approach, *Nonlinearity* **16**: 1751–1791.

[23] Broer, H. W., Huitema, G. B. and Sevryuk, M. B. 1996. Quasi-periodic motions in families of dynamical systems, order amidst chaos, *LNM* **1645**, Springer-Verlag.

[24] Broer, H. W., Huitema, G. B., Takens, F. and Braaksma, B. L. J. 1990. Unfoldings and bifurcations of quasi-periodic tori, *Mem. AMS* **83**(421): 1–175.

[25] Broer, H. W. and Krauskopf, B. 2000. Chaos in periodically driven systems. In B. Krauskopf and D. Lenstra (eds.), *Fundamental Issues of Nonlinear Laser Dynamics*, American Institute of Physics Conference Proceedings **548**: 31–53. ISBN 1-56396-977-7.

[26] Broer, H. W., Naudot, V. and Roussarie, R. 2006. Catastrophe theory in Dulac unfolding, *preprint*.

[27] Broer, H. W., Naudot, V., Roussarie, R. and Saleh, K. 2005. A predator-prey model with non-monotonic response function. To appear *RCD* 2005.

[28] Broer, H. W., Naudot, V., Roussarie, R. and Saleh, K. 2005. Bifurcations of a predator-prey model with non-monotonic response function, *C.R. Acad.Sci. Paris* Ser. I **341**: 601–604.

[29] Broer, H. W., Naudot, V., Roussarie, R. and Saleh, K. 2006. Dynamics of a predator-prey model with non-monotonic response function, *preprint*.

[30] Broer, H. W., Simó, C. and Tatjer, J. C. 1998. Towards global models near homoclinic tangencies of dissipative diffeomorphisms, *Nonlinearity* **11**: 667-770.

[31] Broer, H.W., Simó, C. and Vitolo, R. 2002. Bifurcations and strange attractors in the Lorenz-84 climate model with seasonal forcing, *Nonlinearity* **15**(4): 1205-1267.

[32] Broer, H.W., Simó, C. and Vitolo, R. 2005. Chaos and quasi-periodicity in diffeomorphisms of the solid torus, *Proceedings ENOC*, Eindhoven.

[33] Broer, H.W., Simó, C. and Vitolo, R. 2005. The Hopf-Saddle-Node bifurcation for fixed points of 3D-diffeomorphisms, a dynamical inventory, *submitted*.

[34] Broer, H.W., Simó, C. and Vitolo, R. 2005. The Hopf-Saddle-Node bifurcation for fixed points of 3D-diffeomorphisms, analysis of a resonance 'bubble', *preprint*.

[35] Broer, H. W. and Takens, F. 1989. Formally symmetric normal forms and genericity, *Dynam. Rep.* **2**: 39–59.

[36] Broer, H. W. and Vegter, G. 1992. Bifurcational aspects of parametric resonance, *Dynam. Rep.* (New Series) **1**: 1–53.

[37] Cartwright, M. L. and Littlewood, J. E. 1945. On nonlinear differential equations of the second order, I: The equation $\ddot{y} + k(1 - y^2)\dot{y} + y = b\lambda k \cos(\lambda t + a)$, k large, *Journal of the London Mathematical Society* **20**: 180–189.

[38] Chenciner, A. 1985. Bifurcations de points fixes elliptiques. I. Courbes invariantes, *IHES–Publications mathématiques* $\mathbf{61}$: 67-127.

[39] Chenciner, A., 1985. Bifurcations de points fixes elliptiques. II. Orbites periodiques et ensembles de Cantor invariants, *Inventiones mathematicae* $\mathbf{80}$: 81–106.

[40] Chenciner, A. 1988. Bifurcations de points fixes elliptiques. III. Orbites periodiques de 'petites' périodes et élimination résonnante des couples de courbes invariantes, *IHES–Publications mathématiques* $\mathbf{66}$: 5–91.

[41] Ciocci, M. C., Litvak-Hinenzon, A. and Broer, H. W. 2005. Survey on dissipative KAM theory including quasi-periodic bifurcation theory based on lectures by Henk Broer, to appear in J. Montaldi and T. Ratiu (eds.): *Peyresq Lectures in Geometric Mechanics and Symmetry*, vol. 1. LMS Lecture Notes Series 306 Cambridge University Press.

[42] Doedel, E. J., Champneys, R. A., Fairgrieve, T. F., Kuznetsov, Y. A., Sandstede, B. and Wang, X. J. 2000. *AUTO2000: Continuation and Bifurcation Software for Ordinary Differential Equations (with HomCont), User's Guide*, Concordia University, Montreal, Canada 1997-2000. (http//indy.cs.concordia.ca).

[43] Dumortier, F., Roussarie, R. and Sotomayor, J. 1987. Generic 3-parameter families of vector fields on the plane, unfolding a singularity with nilpotent linear part. The cusp case of codimension 3, *Ergod. Th. & Dynam. Sys.* $\mathbf{7}$: 375-413.

[44] Dumortier, F., Roussarie, R., Sotomayor, J. and Zoladek, H. 1991. Bifurcations of planar vector fields, *LNM* **1480**, Springer Verlag.

[45] Gambaudo, J. M. 1985. Perturbation of a Hopf bifurcation by an external time-periodic forcing, *Journ. Diff. Eqns.* $\mathbf{57}$: 172-199.

[46] Gaunersdorfer, A., Hommes, C. and Wagener, F. O. O. 2000. *Bifurcation routes to volatility clustering*, CeNDEF Working paper WP 00–04.

[47] Gaunersdorfer, A., Hommes, C. H. and Wagener, F. O. O. 2005. Nonlocal onset of instability in an asset pricing model with heterogeneous agents, In: Dumortier, F., Broer, H.W., Mawhin, J., Vanderbauwhede, A. and Verduyn Lunel, S. (eds.), *Proceedings of EQUADIFF 2003*, World Scientific: 613–618.

[48] Gause, G. F. 1932. Experimental studies on the struggle for existence: I. Mixed population of two species of yeast, *J. Exp. Biol.* **9**, 389–390.

[49] Golubitsky, M. and Schaeffer, D. G. 1985. *Singularities and Groups in Bifurcation Theory* Volume I, Appl. Math. Sc. **51**. Springer-Verlag.

[50] Golubitsky, M., Schaeffer, D. G. and Stewart, I. 1988. *Singularities and Groups in Bifurcation Theory* Volume II, Appl. Math. Sc. **69**. Springer-Verlag.

[51] Govaerts, W., Kuznetsov, Y. A. and Dhooge, A. 2005. Numerical continuation of bifurcations of limit cycles in MATLAB, *SIAM J. Sci. Comp.* **27**: 231–252.

[52] Guckenheimer, J. and Holmes, P. 1990. *Nonlinear Oscillations, Dynamical Systems, and Bifurcations of Vector Fields*, Springer-Verlag.

[53] Hanselman, D. 2001. *Mastering Matlab*, University of Maine. (http://www.mathworks.com).

[54] Hanßmann, H. 1998. The quasi-periodic centre-saddle bifurcation, *Journ. Diff. Eqns.* **142**: 35–70.

[55] Holling, C. S. 1959. Some characteristics of simple types of predation and parasitm, *Can. Entomolog.* **91**: 385–398.

[56] Holmes, P. and Rand, D. 1978. Bifurcations of the forced Van der Pol oscillator, *Q. Appl. Math.* **35**: 495–509.

[57] Jorba, À and Simó, C. 1996. On quasi-periodic perturbations of elliptic equilibrium points, *SIAM J. Math. Anal.* **27**: 1704–1737.

[58] Jorba, À and Villanueva, J. 1997. On the persistence of lower-dimensional invariant tori under quasi-periodic perturbations, *J. Nonlinear Sci.* **7**: 427–473.

[59] Krauskopf, B. 1994. Bifurcation sequences at 1:4 resonance: an inventory, *Nonlinearity* **7**(3): 1073–1091.

[60] Krauskopf, B. 2001. Strong resonances and Takens's Utrecht preprint, In H.W. Broer, B. Krauskopf, and G. Vegter (Eds.), *Global Analysis of Dynamical Systems, Festschrift dedicated to Floris Takens for his 60th birthday*, Institute of Physics, Bristol and Philadelphia: 89–111.

[61] Krauskopf, B. and Oldeman, B. 2004. A planar model system for the saddlenode Hopf bifurcation with global reinjection, *Nonlinearity* **17**: 1119–1151.

[62] Krauskopf, B. and Rousseau, C. 1997. Codimension-three unfoldings of reflectionally symmetric planar vector fields, *Nonlinearity* **10**(5): 1115–1150.

[63] Kuznetsov, Y. A. 1995. *Elements of Applied Bifucations Theory*, Springer-Verlag.

[64] Lorenz, E. N. 1984. Irregularity: a fundamental property of the atmosphere, *Tellus A* **36**: 98–110.

[65] Lotka, A. J. 1925. *Elements of Physical Biology*, Williams and Wilkins, Baltimore MD.

[66] Milnor, J. W. 1990. *Topology from Differential Viewpoint*, The University Press of Virginia.

[67] Mora, L. and M. Viana, M. 1993. Abundance of strange attractors, *Acta Math.* **171**: 1–71.

[68] Moser, J. 1965. Combination tones for Duffing's equation, *Comm. Pure Appl. Math.* **18**: 167–181.

[69] Munkres, J. R. 1963. *Elementary Differential Topology*, Princeton Universtity Press.

[70] Norris, J. W. 1993. The closing of Arnol'd tongues for a periodically forced limit cycle, *Nonlinearity* **6**: 1093-1114.

[71] Palis, J. and de Melo, W. 1982. *Geometric Theory of Dynamical Dystem*, Springer-Verlag.

[72] Palis, J. and Takens, F. 1993. Hyperbolicity and sensitive chaotic dynamics at homoclinic bifurcations, *Cambridge Studies in Advanced Mathematics* **35**, Combridge University press.

[73] Rinaldi, S., Muratori, S. and Kuznetsov, Y. A. 1993. Multiple attractors, catastrophes and chaos in seasonally perturbed predator-prey communities, *Bull. Math. Biol.* **55**: 15–35.

[74] Saleh, K. 2005. Organising centres in the semi-global analysis of dynamical systems, *Phd Thesis*, University of Groningen.

[75] Saleh, K. and Wagener, F. O. O. 2005. Semi-global analysis of normal-internal $k : 1$ resonances, *preprint*.

[76] Salomon, E. 1949. The natural control of animal populations, *J. of Anim. and Eco.* **18**: 1-35.

[77] Sanders, J. A. and Verhulst, F. 1985. Averaging methods in nonlinear dynamical systems, *App. Math. Sci.*, Vol. 59, Springer-Verlag.

[78] Shilnikov, A., Nicolis, M. and Nicolis, C. 1995. Bifurcation and predictability analysis of a low-order atmospheric circulation model, *Int. J. bif. & chaos* **5**(6): 1701–1711.

[79] Stoker, J. J. 1950. *Nonlinear Vibrations in Mechanical and Electrical Systems*, Interscience.

[80] Takens, F. 1974. Singularities of Vector Fields, *Publ. Math. IHES* **43**: 47–100.

[81] Takens, F. 2001. Forced oscillations and bifurcations, *Applications of global analysis I* Communications of the Mathematical Institute Rijksuniversiteit Utrecht **3** (1974), 1-59. In H.W. Broer, B. Krauskopf, and G. Vegter (Eds.), *Global Analysis of Dynamical Systems,*

Festschrift dedicated to Floris Takens for his 60th birthday, Institute of Physics, Bristol and Philadelphia: 89–111.

[82] Thom, R. 1993. Structural Stability and Morphogenesis: an Outline of a General Theory of Models, *Reading, MA: Addison-Wesley*.

[83] van Veen, L. 2002. Time scale interaction in low-order climate models, *PhD Thesis*, University of Utrecht.

[84] Vance, W. and Ross, J. 1989. A detailed study of a forced chemical oscillator: Arnol'd tongues and bifurcation sets, *J. Chem. Phys.* **91**(12): 7654–7670.

[85] Vitolo, R. 2003. Bifurcations of attractors in 3D diffeomorphisms, a study in experimental mathematics, *PhD Thesis*, University of Groningen.

[86] Volterra, V. 1926. Variazioni e fluttuaziono del numero di individui in specie animali conviventi, *Mem. Accad. Lincei.* **2**: 31–113.

[87] Wagener, F.O.O. 2001. Semi-local analysis of the $k:1$ and $k:2$ resonances in quasi-periodically forced system, In H.W. Broer, B. Krauskopf, and G. Vegter (Eds.), *Global Analysis of Dynamical Systems, Festschrift dedicated to Floris Takens for his 60th birthday*, Institute of Physics, Bristol and Philadelphia: 113–129.

[88] Wagener, F. O. O. 2002. On the quasi-periodic d-fold degenerate bifurcations, *preprint*.

[89] Wagener, F. O. O. 2003. Skiba points and heteroclinic bifurcations, with applications to the shallow lake system, *Journal of Economic Dynamics and Control* **27**: 1533–1561.

[90] Wagener, F. O. O. 2005. Structural analysis of optimal investment for firms with non-concave revenues, *Journal of Economic Behavior and Organisation* **57**: 474–489.

[91] Wagener, F. O. O. 2003. A Gevrey regular KAM theorem and the inverse approximation lemma, *Dynamical systems, an international journal* **18**(2): 159–163(5).

[92] Whitney, H. 1955. On singularities of mappings of Euclidean spaces. I. Mappings of the plane into the plane, *Ann. Math.* II. Ser. 62: 374-410.

[93] Wolfram, S. 1996. *The Mathematica book*, Cambridge University Press, Wolfram research Inc. (http://www.wolfram.com).

[94] Zeeman, E. C. 1977. Catastrophe Theory, *Selected Papers 1972–1977*, Reading, MA: Addison-Wesley.

[95] Zhu, H., Campbell, S. A. and Wolkowicz, G. S. K. 2002. Bifurcation analysis of a predator-prey system with nonmonotonic functional response, *Siam J. Appl. Math.* **63**: 636–682.